Asian Journal of Surgery (2019) 42, 947–956

Available online at www.sciencedirect.com

ScienceDirect

journal homepage: www.e-asianjournalsurgery.com

ORIGINAL ARTICLE

Mechanical effect of different implant caput-collum-diaphyseal angles on the fracture surface after fixation of an unstable intertrochanteric fracture: A finite element analysis

Jung-Taek Kim [a], Chang-Ho Jung [b], Quan Hu Shen [a,c], Yong-Han Cha [d], Chan Ho Park [e], Jun-Il Yoo [f], Hyung Keun Song [a], Yongho Jeon [b], Ye-Yeon Won [a,*]

[a] *Department of Orthopaedic Surgery, Ajou University School of Medicine, Ajou Medical Center, Suwon, South Korea*
[b] *Department of Mechanical Engineering, Ajou University, Suwon, South Korea*
[c] *Department of Orthopaedics, First People's Hospital of Suqian City, Jiangsu, China*
[d] *Department of Orthopaedic Surgery, Eulji University Hospital, Daejeon, South Korea*
[e] *Department of Orthopaedic Surgery, Yeungnam University Medical Center, Daegu, South Korea*
[f] *Department of Orthopaedic Surgery, Gyeongsang National University Hospital, Jinju, South Korea*

Received 13 September 2018; received in revised form 24 November 2018; accepted 23 January 2019
Available online 20 February 2019

KEYWORDS
Hip fracture;
Fracture fixation;
Proximal femoral nail antirotation;
Finite element analysis

Summary *Background/Objective:* The choice of implant is one of the most easily controllable factors affecting the outcome of intertrochanteric fractures. While most of the caput-collum-diaphysis (CCD) angles of the femur are within the range of 125° and 130°, there is a shortage of data on whether 125° or 130° implants are preferable. Thus, the present finite element analysis (FEA) aimed to compare the biomechanical effects on the fracture surface when using implants with different CCD angles where the anatomical CCD angle of the femur was between 125° and 130°.
Methods: After establishing a finite element model of an unstable intertrochanteric fracture from the femur with a native CCD angle of 127.3°, proximal femoral nail antirotation (PFNA) models with CCD angles of 125° and 130° were virtually implanted to have the same position of screw tip, respectively.

* Corresponding author. Department of Orthopedic Surgery, Ajou University School of Medicine, Ajou University Medical Center, 164, World cup-ro, Yeongtong-gu, Suwon-si, Gyeonggi-do, 16499, South Korea. Fax: +82 31 219 5229.
E-mail address: thrtkr@ajou.ac.kr (Y.-Y. Won).

https://doi.org/10.1016/j.asjsur.2019.01.008

Results: In the one-leg stance during walking, when the implant with 130º CCD angle was used, the magnitude of compressive stress (1.61 and 2.12 MPa in the 130° and 125° model, respectively) was lower and the area of the fracture surface under tensile stress (55% and 5% in 130° and 125° model, respectively), the interfragmentary movements (40.9% more movement in 130° model), and the magnitude of bone deformation (23.5% more deformation in 130° model) were more than those of the 125° model.
Conclusion: The intertrochanteric fracture fixed with PFNA with a 125º CCD angle revealed less interfragmentary movement on the fracture surface when the native CCD was an in-between angle in the FEA.

1. Introduction

Hip fracture is one of the most common medical issues encountered by orthopaedic surgeons. The International Osteoporosis Foundation reported that there are approximately 1.6 million hip fractures globally each year and predicted that this would increase to 4.5 million by 2050.[1–3]

Among various types of hip fractures, unstable trochanteric fractures are a great burden to society and cause major problems worldwide.[4–11] Failure rates are higher (8%–25%) with unstable fracture patterns[12] and are as high as 50% in the most unstable fractures.[13]

While the sliding hip screw (SHS) is the implant of choice in stable intertrochanteric fractures, intramedullary devices have been used for over 25 years, and they are the preferred treatment method used by orthopaedic surgeons for unstable intertrochanteric fractures.[14] Practice guidelines from the American Association of Orthopaedic Surgery (AAOS) also recommend the use of an intramedullary device.[2,15,16]

Various factors are known to affect the outcomes of unstable intertrochanteric fracture treatment, including fracture type, bone quality of the affected limb, activity level before fracture, the position of the lag screw or the helical blade within the femoral head, the quality of reduction, choice of implant, surgeon's familiarity with a specific implant, distal locking, and length of the nail.[2,17] As the outcome of treatment is multifactorial, the modifiable factors have been discussed for better outcomes, with implant choice being one of the major discussion topics.[2,18]

Anatomical studies reported that the caput-collum-diaphysis (CCD) angle of the femur varies with ethnic differences.[19–21] Despite the variation, most of the mean values were within the range of 125°–130°.[4,19,20,22] Most manufacturers of intramedullary devices provide two or more options for implant CCD angles to help surgeons to cope with anatomical variations in patients, following the results of anatomical studies. As the mean CCD angle of the femur is 127° with a standard deviation of 5°, one can estimate that about 38% of patients should be within the range of 125° and 130°.

For femurs with an in-between angle, even after anatomical reduction of the fracture and positioning of the screw tip in the central area in the anterior/posterior and lateral planes, as is typically recommended, implants with a 125° or a 130º CCD angle are acceptable[21,23,24] (Fig. 1). Nevertheless, it is difficult to decide between these two angles, due to the paucity of helpful information in previous studies.

We postulated that if the CCD angle of the femur had in-between selectable options, the implant with a higher CCD angle would provide better stability as bending component of physical load would be less than that of a lower CCD angle.

Therefore, the aim of the present study was to compare the biomechanical effects of intramedullary fixations with

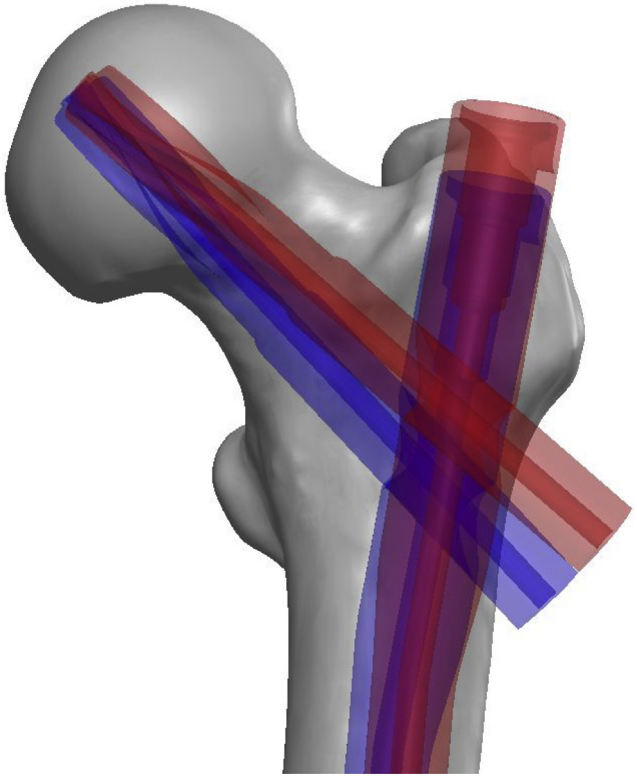

Figure 1 In a femur with an in-between angle, it is acceptable to use implants with a caput-collum-diaphysis (CCD) angle of either 125° or 130° after anatomical reduction of the fracture, even if the screw tip is positioned in the centre of the head in the anterior/posterior and lateral planes, which is typically recommended.

different CCD angles were used in cases where the anatomical CCD angle of the femur was between 125° and 130°.

2. Methods

The requirement for informed consent was waived by the Institutional Review Board of our hospital as performing CT was part of routine care and the use of these data posed minimal risk to patients.

Since there are several factors affecting the treatment outcomes of intertrochanteric fracture, it is difficult to control all other factors in a clinical study and only observe the effects of a single variable. Thus, we designed this experiment as a finite element analysis (FEA) study.[2,17,18]

2.1. Three-dimensional modelling of the femur

An angio-CT scan performed to evaluate deep vein thrombosis in a 78-year-old patient with a right intertrochanteric fracture was used for this simulation. The patient was selected as the CCD angle of his femur was 127.3° in the 3-dimensional (3D) CT, which is close to the mean value of Korean femurs.[19]

In terms of basic anthromorphometric information, the patient's height and weight were 165 cm and 59.6 kg, respectively.

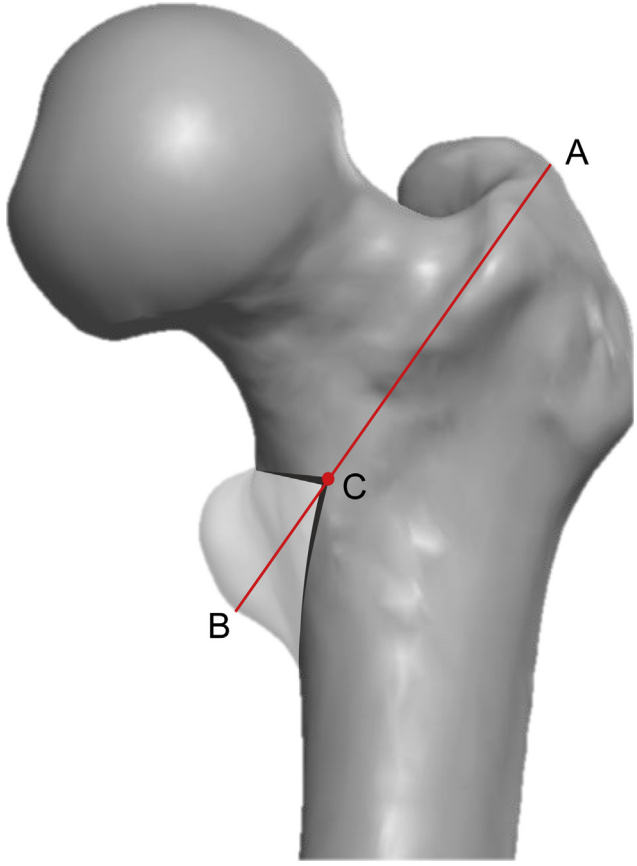

Figure 2 A model of unstable intertrochanteric fracture was established, corresponding to the Muller AO classification 31-A2.1[24], with 30% defect (BC/AB) in the medial support fragment at the level of the lesser trochanter.[25]

MIMICS Research 20.0 (Materialise Interactive Medical Image Control System; Materialise, Antwerp, Belgium) was used to reconstruct 3D models of the femur from the CT images.

2.2. Fracture models

Using virtual osteotomy, we established a model of unstable intertrochanteric fracture corresponding to the Muller AO classification 31-A2.1 (unstable fracture type), with no medial support at the level of the lesser trochanter.[25,26]

We assumed that the angle of the fracture line relative to the femoral anatomic axis was 30°, and the defect in the medial support fragment was 30%[26] (Fig. 2).

2.3. Implant model

The 3D PFNA-II model (Ø 10 mm; AO Synthes, Swiss) as stereo-lithograph (STL) format was created using 3D Scanner (Rainbow Scanner Prime; Dentium, Seoul, Korea) and Micro CT (SkyScan1173; Bruker-CT, Belgium) Scanning. The implant model was reconstructed into 3-dimensional data by comparing the model data acquired through the 3D scanner and the Micro CT with Nrecon (Bruker-CT) and Creo 2.0 (PTC, Boston, USA).

2.4. Coordinate system

The coordinate system for the femur applied in this study is based on the definition by Bergmann et al[27] The femoral shaft axis defines the z-axis of the global coordinate system. The x-axis lies in the frontal plane as mapped by the shaft axis and the femoral neck axis. The y-axis completes the right-hand system.[27]

2.5. Implant positioning

The 3D model of implant was virtually implanted into the 3D model of the femur using Creo 2.0.

To compare the effect of the CCD angle of the implant to the fracture surface, two models of femur-implant composite were created. An implant model with a 125° CCD angle was virtually implanted to the 125° model while one with a 130° CCD angle was used to form the 130° model. These two models were identical in terms of tip apex distance (TAD), reduction quality, implant type, fracture pattern, and patient factors, including material property of bone and femoral geometry[23,28,29] (Fig. 1).

The implant position was controlled by placing the tip of blade at the same point in both models which was known as the ideal position of spiral blade (centre—centre position) and placing the nail without lateral cortex impingement of the proximal femur in the coronal view and anterior cortex impingement in the sagittal view.[23] The tip of blade was positioned 7 mm below the subchondral bone to yield a tip apex distance of 14 mm according to literature and surgical guide.[23]

We utilized Boolean subtraction to recreate the drilling and reaming process used to insert the nail into the femur.[30]

2.6. Solver

ANSYS Ver. 18.0 software with academic license (ANSYS Inc., Canonsburg, PA, USA) was used. The mesh of the models was generated using the tetrahedrons element type (Fig. 3). The finite element model had 239,731 nodes and 156,281 elements. While the mesh size was adjusted to 4 mm, the fracture surface was given a fine mesh, which was 1 mm for more detailed results.

2.7. Boundary conditions

All contacts between the two fracture fragments and the implant were considered. All contacts were modelled as frictional contacts. The femur was fixed from the distal condylar articular face. Friction coefficient is 0.46 for bone—bone interactions, 0.42 for bone-implant interactions, and 0.2 for implant—implant interactions.[31]

Both the bone and the implant were assumed to be composed of isotropic and linearly elastic materials. Bone was considered homogeneous material, for which elastic modulus and Poisson's ratio were respectively assigned to the values of 17.5 GPa and 0.3.[32—34] The proximal femoral nail antirotation (PFNA) was considered to be made of titanium alloy (Ti-6Al-7Nb) with an elastic modulus of 105 GPa and a Poisson's ratio of 0.34.[35]

2.8. Loading condition

Bodyweight loading forces were applied according to Bergmann et al.[27]

During the recovery phase after hip surgery, climbing or descending stairs accounts for 0.4% of all activity, whereas walking accounts for 10.2%. Therefore, we used a one-leg stance during walking as the loading condition.[36]

A resultant load vector of 1752.2 N corresponded to 300% for a bodyweight of 59.6 kg at an angle of 24° in the frontal plane and 17° in the axial plane (Fig. 4a).[27,31] Abductor force was applied on the greater trochanter.[31] We assumed that the weight load was transferred to the surface of hemisphere, which was inclined 45 and retroverted 25' with the consideration of the inclination of acetabulum and the anteversion of both femur and acetabulum[19,20,37] (Fig. 4b).

To evaluate the accuracy of our finite element models, a convergence test of total strain energy was performed. With these settings, the analysis was performed based on the convergence results without any special error.

2.9. Biomechanical effects on the fracture surface

Stress on the fracture surface was compared in aspect of normal stress on fracture surface, ratio of the area with compressive stress to that with tensile stress, average compressive stress on fracture surface, and the distribution of shear stress were evaluated on the fracture surface.[38—44]

The interfragmentary gap after loading was calculated and compared.[45,46]

To compare the stability between femur-implant constructs of both models, bone deformation after loading was compared.

3. Results

Normal stress distribution maps in the fracture surface are shown in Fig. 5a for both models. Higher maximum compressive stress was found in the 130° model (140.6 MPa) compared to the 125° model (63.2 MPa), while peak tensile stress was 25.3 MPa in the 125° model and 15.6 MPa in the 130° model.

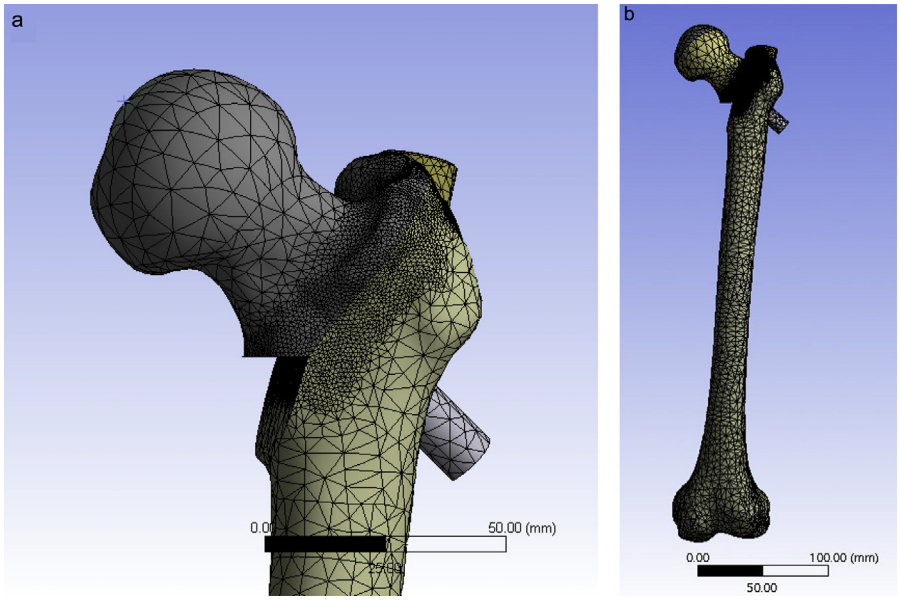

Figure 3 A finite element model of unstable intertrochanteric fracture fixed with Proximal Femoral Nail Antirotation (PFNA) of 125 ° CCD angle. a. A total of 156,281 tetrahedral elements constitutes the femur model with 239,731 nodes. b. While the mesh size was adjusted to 4 mm, the fracture surface was given a fine mesh, which was 1 mm for more detailed results.

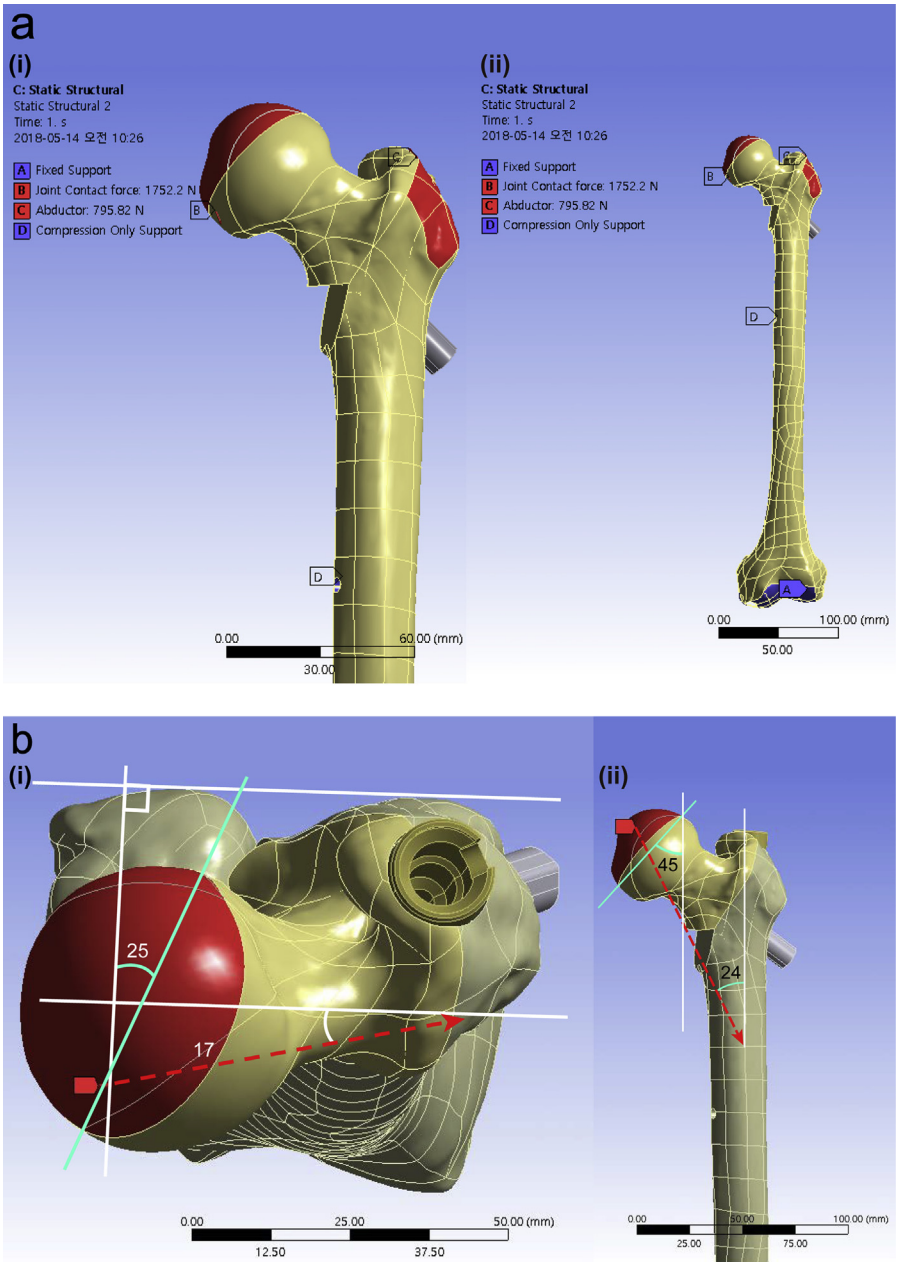

Figure 4 Loading condition. a. Load vector of 1752.2 N corresponds to 300% for a bodyweight of 59.6 kg. Abductor force was applied on the greater trochanter. b. Load vector (red dashed arrow) had an angle of 24° in the frontal plane and 17° in the axial plane.[26] Weight load (green solid line) was transferred to the surface of hemisphere at an incline of 45° and retroversion of 25°.

When the area with compressive stress was mapped in each model (Fig. 5b), 95.1% of the fracture surface was under compressive stress in the 125° model while 55% of the fracture surface was under compressive stress in the 130° model.

The average compressive stress on the fracture surface was 2.12 MPa in the 125° model and 1.61 MPa in the 130° model, meaning that the compressive stress on the fracture surface was higher in the 125° model (Table 1). The distribution of shear stress in the fracture surface was similar in both models (Fig. 5c).

The interfragmentary gap after loading of 130° model was 40.9% larger than that of 125° model (0.34 mm in 125° model, and 0.48 mm in 130° model; Fig. 5d).

A comparison of the bone deformation of the femur head was shown in Fig. 5e. More bone deformation was observed in the 130° model than in the 125° model. Maximum bone deformation in the 130° model was 23.5% larger than that of the 125° model. (2.1 mm in the 130° model, and 1.7 mm in the 125° model; Fig. 5e).

4. Discussion

As the choice of implant is an easily controllable factor among the various factors that affect the mechanical environment of fracture fixation, various fixation devices have been designed and compared among themselves. Intramedullary devices were compared to extramedullary

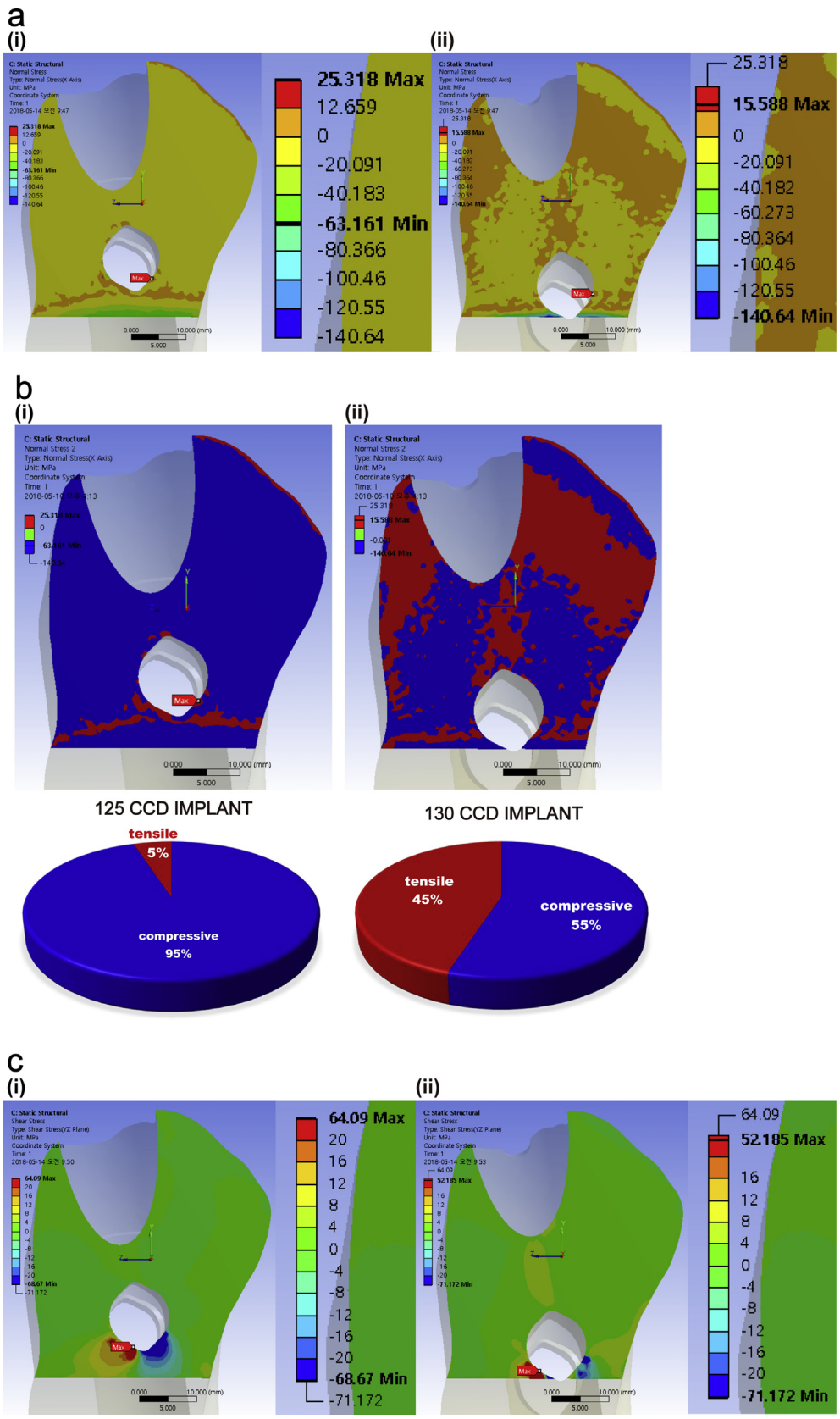

Figure 5 Mechanical environment of fracture surface was estimated. In each figure, (i) represents 125° model, (ii) represents 130° model. a. normal stress distribution. b. area of compressive and tensile stress. c. shear stress distribution. d. interfragmentary gap with loading. e. deformation after loading.

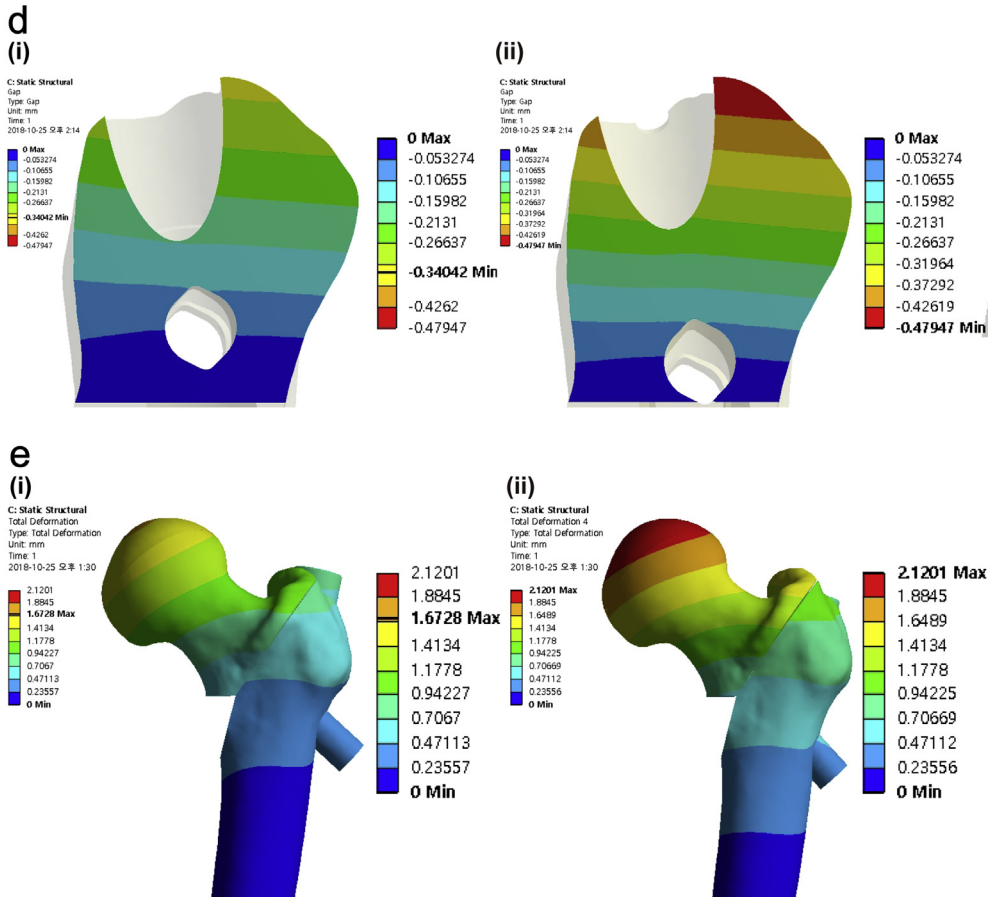

Figure 5 (*continued*).

Table 1 Average compressive stress on the fracture surface.

Parameters of fracture surface	125°	130°
Area (mm^2)	1206.3	1232.2
Compressive stress (N)	2561.8	1984.7
Average compressive stress (MPa)	2.12	1.61

ones, and screw type lag screws were compared to blade type ones, 2 screw systems were compared to 1 screw systems.[11,28,47–49] However, few studies compared the effects of different CCD angles of implants when multiple CCD angles are applicable. Given the anatomical study regarding femoral CCD angle, it is not rare for surgeons to face situations in which they must choose one of applicable CCD angles of ready-made implants.[4,19,20]

In this study, we used 3-D models of implants with a CCD angle of 125° and 130° to virtually fix an unstable intertrochanteric fracture model in a patient with a native CCD angle of 127° and then used FEA to compare the mechanical effects at the fracture surface during walking.

Mechanical environment for fracture stability was assessed in three main features. Compression on the fracture surface has an additive effect for fracture healing, whereas tension and shear inhibit fracture repair.[50] Various fixation devices have been designed to provide better mechanical environment for fracture healing; the key concept of these devices has been controlled compression at the fracture site.[18] Previous finite element studies for fracture fixation also evaluated the area with compression.[31,39] Interfragmentary movement is one of the major mechanical factors of fracture healing.[45,46] The difference of deformation with the same loading condition indicates the stability of fractured femur-implant construct.[51] When the implant with 125° CCD angle was used, the area of the fracture surface under compressive stress and the magnitude of compressive stress were more and the interfragmentary movements and the magnitude of deformation were less than those in the 130° model. It demonstrated that unstable intertrochanteric fracture model fixed with implants with a CCD angle of 125° was more mechanically stable construct than that with 130 ° CCD implant.

As the purpose of the present study was to compare plainly the mechanical effects of two CCD angles of implants, several factors were simplified based on previous finite element studies.[33,34,52] Although natural bone is heterogenous, anisotropic, and nonlinear material, the femur was modelled as a homogenous, isotropic, and linearly elastic material.[53] A simplified fracture surface consisted of one plane. Additionally, the fracture gap cannot be absent in a real situation, though a perfect reduction was assumed to control the reduction quality. However, the relative difference between two models of the present study provided insight for the comparison.

Contrary to the intuitive hypothesis, several mechanical factors provide the 125° model with advantages. When the blade tip is located at the same ideal location, the difference in the implant CCD angle is thought to cause several mechanical discrepancies, which then causes the difference in mechanical environment at the fracture surface. Given the same reduction quality, when a walking load is applied, the stress in the direction of the blade sliding was larger for the 130° implant (Fig. 6a). The blade undergoes stress that bends the head medially, and in turn forms a moment that rotates the proximal fragment in the medial direction, with the length of the blade acting as the lever arm length (Fig. 6b). Differences in the depth of the nail cause differences in the distance between the rotation centre and the fracture surface. Since the distance between the nail and the fracture surface is greater in the 130° model than the 125° model, the forces acting on the fracture surface are different, even given the same moment (Fig. 6c). Given the same tip position, because the CCD angle of the implant determines the path of the blade, this results in different amounts of medial buttressing bone. The 125° model had a greater amount of medial buttressing bone than the 130° model (Fig. 6d). On summary, differences in the implant CCD angle determined not only the sliding direction of the blade, but also the blade length, the nail depth, the distance from the medial cortex to the blade, and the amount of buttressing bone medial to the blade at the fracture surface; in combination, these factors resulted in better mechanical conditions for the 125° model.

Few studies have been conducted regarding the effect of the implants' CCD angles on the fracture fixation. In a retrospective study, fixation of unstable intertrochanteric fractures with an implant's CCD angle less than the native CCD angle was associated with more varus reductions and fracture displacement. No significant correlation was observed with lag screw cutout.[24] However, the study had many limitations. Exclusion of 71 out of 154 subjects introduces a risk of sampling bias, and since 84% of subjects only received implants with a CCD angle of 125°, other angles were severely underrepresented. Due to the low number of cases showing treatment failure, statistical comparison was difficult; in addition, there was no assessment of reduction quality prior to fixation, and hence it was difficult to tell whether the trend for varus reductions was affected by the choice of implant. Because there are multiple factors that determine the outcomes of intertrochanteric fracture, the effects of any one factor of interest can only be ascertained by focusing on that factor. In that previous study, the reliability of the native CCD angle measurements was not mentioned, casting further doubt on the reliability of the conclusions. Because most studies have not evaluated this relationship, it is thought that it remains uncertain. In the future, it will be necessary to study real cases in a well-controlled environment.

We acknowledge that our study has several limitations. Because the finite element analysis is based on various assumptions for simplification, the results of the present study may only be used to infer the effects of the implant

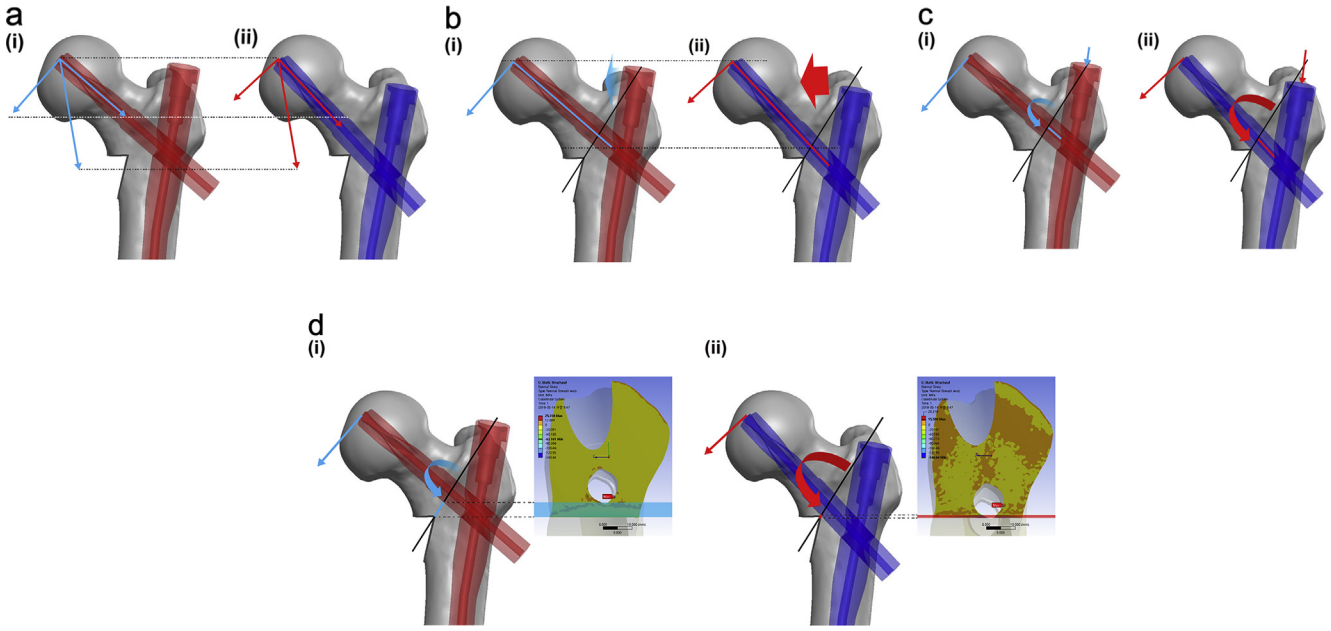

Figure 6 Differences in the implant CCD angle lead to differences in the direction of blade sliding and in the blade length, the nail depth, the distance from the medial cortex to the blade, and the amount of buttressing bone medial to the blade at the fracture surface. Due to a combination of these effects, the 125° model showed better mechanical conditions at the fracture surface. In each figure, (i) represents the 125° model, (ii) represents the 130° model. a. The force component in the direction of blade sliding was larger when using the 130° model. b. The blade length, which acts as the lever arm length in the moment causing medial rotation of the proximal fragment, was larger in the 130° model. c. The nail was deeper in the 130° model, meaning that there was a greater distance between the nail and the fracture surface. d. The 125° model showed more medial buttressing bone (blue shadow in 125° model, red shadow in 130° model) than the 130° model.

CCD angles. Although the femur was modelled from an elderly patient who suffered from intertrochanteric fracture, we assumed that the femur was composed of a homogenous, isotropic, and elastic material. As the goal is a comparative biomechanical analysis, the mean features would be adequate.[34] In this study, experimental validation was not made. Instead, validity of the FE model was accepted by making the convergence study.

5. Conclusion

In the present FEA, intertrochanteric fracture fixed with PFNA with a 125º CCD angle revealed a better biomechanical environment on the fracture surface than that with a 130 º CCD angle when the native CCD was an in-between angle.

Conflicts of interest and source of funding

The authors have no competing interests.

Acknowledgment

We thank the company Dentium (Seoul, Korea) for assistance with reconstruction and virtual surgery with 3D models using MIMICS Research 20.0, Nrecon, and Creo 2.0.

References

1. International Osteoporosis Foundation: Hip Fracture [IOF web site]. Available at: https://www.iofbonehealth.org/facts-statistics#category-16. Accessed 17 August 2018.
2. Socci AR, Casemyr NE, Leslie MP, Baumgaertner MR. Implant options for the treatment of intertrochanteric fractures of the hip: rationale, evidence, and recommendations. *Bone Joint J*. 2017;99-B:128–133.
3. Gullberg B, Johnell O, Kanis JA. World-wide projections for hip fracture. *Osteoporos Int*. 1997;7:407–413.
4. Sawaguchi T, Sakagoshi D, Shima Y, Ito T, Goldhahn S. Do design adaptations of a trochanteric nail make sense for Asian patients? Results of a multicenter study of the PFNA-II in Japan. *Injury*. 2014;45:1624–1631.
5. Lindskog DM, Baumgaertner MR. Unstable intertrochanteric hip fractures in the elderly. *J Am Acad Orthop Surg*. 2004;12:179–190.
6. Veronese N, Maggi S. Epidemiology and social costs of hip fracture. *Injury*. 2018;49:1458–1460.
7. Taguchi Y, Inoue Y, Kido T, Arai N. Treatment costs and cost drivers among osteoporotic fracture patients in Japan: a retrospective database analysis. *Arch Osteoporos*. 2018;13:45.
8. Gardenbroek TJ, Segers MJ, Simmermacher RK, Hammacher ER. The proximal femur nail antirotation: an identifiable improvement in the treatment of unstable pertrochanteric fractures? *J Trauma*. 2011;71:169–174.
9. Gardner MJ, Bhandari M, Lawrence BD, Helfet DL, Lorich DG. Treatment of intertrochanteric hip fractures with the AO trochanteric fixation nail. *Orthopedics*. 2005;28:117–122.
10. Gotfried Y. The lateral trochanteric wall: a key element in the reconstruction of unstable pertrochanteric hip fractures. *Clin Orthop Relat Res*. 2004:82–86.
11. Parker MJ, Handoll HH. Gamma and other cephalocondylic intramedullary nails versus extramedullary implants for extracapsular hip fractures in adults. *Cochrane Database Syst Rev*. 2010:CD000093.
12. Medoff RJ, Maes K. A new device for the fixation of unstable pertrochanteric fractures of the hip. *J Bone Joint Surg Am*. 1991;73:1192–1199.
13. Haidukewych GJ, Israel TA, Berry DJ. Reverse obliquity fractures of the intertrochanteric region of the femur. *J Bone Joint Surg Am*. 2001;83-A:643–650.
14. Koval KJ. Intramedullary nailing of proximal femur fractures. *Am J Orthop (Belle Mead NJ)*. 2007;36:4–7.
15. Chen F, Wang Z, Bhattacharyya T. Convergence of outcomes for hip fracture fixation by nails and plates. *Clin Orthop Relat Res*. 2013;471:1349–1355.
16. Management of Hip Fractures in the Elderly. [American Academy of Orthopaedic Surgeons]. Available at: http://www.orthoguidelines.org/topic?id=1017. Accessed 17 August 2018.
17. Hsueh KK, Fang CK, Chen CM, Su YP, Wu HF, Chiu FY. Risk factors in cutout of sliding hip screw in intertrochanteric fractures: an evaluation of 937 patients. *Int Orthop*. 2010;34:1273–1276.
18. Babhulkar S. Unstable trochanteric fractures: issues and avoiding pitfalls. *Injury*. 2017;48:803–818.
19. Cho HJ, Kwak DS, Kim IB. Morphometric evaluation of Korean femurs by geometric computation: comparisons of the sex and the population. *Biomed Res Int*. 2015;2015:730538.
20. Chantarapanich N, Rojanasthien S, Chernchujit B, et al. 3D CAD/reverse engineering technique for assessment of Thai morphology: proximal femur and acetabulum. *J Orthop Sci*. 2017;22:703–709.
21. Walton NP, Wynn-Jones H, Ward MS, Wimhurst JA. Femoral neck-shaft angle in extra-capsular proximal femoral fracture fixation; does it make a TAD of difference? *Injury*. 2005;36:1361–1364.
22. Pathrot D, Ul Haq R, Aggarwal AN, Nagar M, Bhatt S. Assessment of the geometry of proximal femur for short cephalomedullary nail placement: an observational study in dry femora and living subjects. *Indian J Orthop*. 2016;50:269–276.
23. Baumgaertner MR, Curtin SL, Lindskog DM, Keggi JM. The value of the tip-apex distance in predicting failure of fixation of peritrochanteric fractures of the hip. *J Bone Joint Surg Am*. 1995;77:1058–1064.
24. Parry JA, Barrett I, Schoch B, Yuan B, Cass J, Cross W. Does the angle of the nail matter for pertrochanteric fracture reduction? Matching nail angle and native neck-shaft angle. *J Orthop Trauma*. 2018;32:174–177.
25. Müller ME, Nazarian S, Koch P, Schatzker J. *The Comprehensive Classification of Fractures of Long Bones*. Springer Science & Business Media; 2012.
26. Celik T, Mutlu I, Ozkan A, Kisioglu Y. Comparison of the lag screw placements for the treatment of stable and unstable intertrochanteric femoral fractures regarding trabecular bone failure. *J Med Eng*. 2016;2016:5470798.
27. Bergmann G, Graichen F, Rohlmann A. Hip joint loading during walking and running, measured in two patients. *J Biomech*. 1993;26:969–990.
28. Sambandam SN, Chandrasekharan J, Mounasamy V, Mauffrey C. Intertrochanteric fractures: a review of fixation methods. *Eur J Orthop Surg Traumatol*. 2016;26:339–353.
29. Haidukewych GJ. Intertrochanteric fractures: ten tips to improve results. *J Bone Joint Surg Am*. 2009;91:712–719.
30. Eberle S, Gerber C, von Oldenburg G, Hungerer S, Augat P. Type of hip fracture determines load share in intramedullary osteosynthesis. *Clin Orthop Relat Res*. 2009;467:1972–1980.
31. Lee PY, Lin KJ, Wei HW, et al. Biomechanical effect of different femoral neck blade position on the fixation of intertrochanteric fracture: a finite element analysis. *Biomed Tech (Berl)*. 2016;61:331–336.
32. Inal S, Taspinar F, Gulbandilar E, Gok K. Comparison of the biomechanical effects of pertrochanteric fixator and dynamic

hip screw on an intertrochanteric femoral fracture using the finite element method. *Int J Med Robot*. 2015;11:95—103.
33. Cegonino J, Garcia Aznar JM, Doblare M, Palanca D, Seral B, Seral F. A comparative analysis of different treatments for distal femur fractures using the finite element method. *Comput Methods Biomech Biomed Eng*. 2004;7:245—256.
34. Oken OF, Soydan Z, Yildirim AO, Gulcek M, Ozlu K, Ucaner A. Performance of modified anatomic plates is comparable to proximal femoral nail, dynamic hip screw and anatomic plates: finite element and biomechanical testing. *Injury*. 2011;42:1077—1083.
35. ASTM F1295-16. *Standard Specification for Wrought Titanium-6 Aluminum-7 Niobium Alloy for Surgical Implant Applications (UNS R56700)*. West Conshohocken, PA: ASTM International; 2016. www.astm.org.
36. Morlock M, Schneider E, Bluhm A, et al. Duration and frequency of every day activities in total hip patients. *J Biomech*. 2001;34:873—881.
37. Ma H, Han Y, Yang Q, et al. Three-dimensional computed tomography reconstruction measurements of acetabulum in Chinese adults. *Anat Rec (Hoboken)*. 2014;297:643—649.
38. Augat P, Burger J, Schorlemmer S, Henke T, Peraus M, Claes L. Shear movement at the fracture site delays healing in a diaphyseal fracture model. *J Orthop Res*. 2003;21:1011—1017.
39. Helwig P, Faust G, Hindenlang U, et al. Finite element analysis of four different implants inserted in different positions to stabilize an idealized trochanteric femoral fracture. *Injury*. 2009;40:288—295.
40. Klein P, Opitz M, Schell H, et al. Comparison of unreamed nailing and external fixation of tibial diastases-mechanical conditions during healing and biological outcome. *J Orthop Res*. 2004;22:1072—1078.
41. Molster AO. Effects of rotational instability on healing of femoral osteotomies in the rat. *Acta Orthop Scand*. 1984;55:632—636.
42. Perren SM. Physical and biological aspects of fracture healing with special reference to internal fixation. *Clin Orthop Relat Res*. 1979:175—196.
43. Sigurdsen U, Reikeras O, Utvag SE. The influence of compression on the healing of experimental tibial fractures. *Injury*. 2011;42:1152—1156.
44. Hente R, Fuchtmeier B, Schlegel U, Ernstberger A, Perren SM. The influence of cyclic compression and distraction on the healing of experimental tibial fractures. *J Orthop Res*. 2004;22:709—715.
45. Augat P, Simon U, Liedert A, Claes L. Mechanics and mechano-biology of fracture healing in normal and osteoporotic bone. *Osteoporos Int*. 2005;16(Suppl 2):S36—S43.
46. Glatt V, Evans CH, Tetsworth K. A concert between biology and biomechanics: the influence of the mechanical environment on bone healing. *Front Physiol*. 2016;7:678.
47. Fang C, Lau TW, Wong TM, Lee HL, Leung F. Sliding hip screw versus sliding helical blade for intertrochanteric fractures: a propensity score-matched case control study. *Bone Joint J*. 2015;97-B:398—404.
48. Sommers MB, Roth C, Hall H, et al. A laboratory model to evaluate cutout resistance of implants for pertrochanteric fracture fixation. *J Orthop Trauma*. 2004;18:361—368.
49. Wu D, Ren G, Peng C, Zheng X, Mao F, Zhang Y. InterTan nail versus Gamma3 nail for intramedullary nailing of unstable trochanteric fractures. *Diagn Pathol*. 2014;9:191.
50. Claes LE, Heigele CA. Magnitudes of local stress and strain along bony surfaces predict the course and type of fracture healing. *J Biomech*. 1999;32:255—266.
51. Hwang JH, Garg AK, Oh JK, et al. A biomechanical evaluation of proximal femoral nail antirotation with respect to helical blade position in femoral head: a cadaveric study. *Indian J Orthop*. 2012;46:627—632.
52. Huiskes R, Chao EY. A survey of finite element analysis in orthopedic biomechanics: the first decade. *J Biomech*. 1983;16:385—409.
53. Wirtz DC, Schiffers N, Pandorf T, Radermacher K, Weichert D, Forst R. Critical evaluation of known bone material properties to realize anisotropic FE-simulation of the proximal femur. *J Biomech*. 2000;33:1325—1330.